



Effect of nanostructured zirconium dioxide incorporation in an experimental adhesive resin

Camila Provenzi¹ · Fabrício Mezzomo Collares¹ · Marla Cuppini¹ · Susana Maria Werner Samuel¹ · Annelise Kopp Alves² · Carlos Pérez Bergmann² · Vicente Castelo Branco Leitune¹

Received: 26 June 2017 / Accepted: 12 December 2017 / Published online: 5 January 2018
© Springer-Verlag GmbH Germany, part of Springer Nature 2018

Abstract

Objectives The aim of this study was to evaluate the influence of nanostructured zirconium dioxide incorporation in an experimental adhesive resin.

Methods ZrO₂ particles were characterized by X-ray diffraction (XRD), micro-Raman spectroscopy and Brunauer–Emmett–Teller (B.E.T). Experimental adhesive resins were formulated with 0, 0.5, 1, 4.8, and 9.1% ZrO₂ in weight. The adhesives were evaluated based on degree of conversion (DC), radiopacity, softening in solvent and microtensile bond strength (μ TBS) 24 h and after 1 year of aging. Mineral deposition at the hybrid layer was assessed with micro-Raman spectroscopy at the baseline and after 14 days.

Results XRD showed monoclinic and tetragonal phases of ZrO₂ particles. B.E.T data revealed a surface area of 37.41 m²/g, and typical chemical groups were shown on the Raman spectra. The addition of ZrO₂ did not influence the radiopacity. The addition of 4.8% and 9.1 wt.% ZrO₂ showed higher initial hardness with increased softening in solvent ($P < 0.05$) and promoted mineral deposition at the dentin interface. DC was significantly increased in the group with 1% ZrO₂ ($P < 0.05$). The μ TBS test showed difference on the group with 9.1 wt.% of ZrO₂, with a significant reduction after aging.

Conclusion The incorporation of ZrO₂ promoted mineral deposition on the adhesive interface and the addition of 1 wt.% caused a significant increase on the DC without compromising the other physicochemical characteristics, which may prove promising for the development of new dental adhesive systems.

Clinical relevance The mineral deposition on the hybrid layer can result in a longer stability of the adhesive, thus delaying the hydrolytic degradation.

Keywords Nanostructures · Zirconium dioxide · Dentin bonding agents

Introduction

In the last decade, the role of the adhesive system components in the adhesion process has been extensively studied [1–3]. A stable bonding of dental adhesives to tooth substrates relies on the mechanical and chemical features of the polymeric material

[4]. However, some concerns regarding the hybrid layer degradation over time, nanoleakage and longevity of materials in the oral environment remain issues to dentin adhesion [5–9]. The development of polymeric materials with better clinical behavior has been the subject of research and of great interest in the scientific community and dental materials industry [10–13].

Several studies have incorporated fillers, such as hydroxyapatite [14], niobium pentoxide [4], tantalum oxide [15], and titanium dioxide [16] into the organic matrix of adhesive resins and improved mechanical properties have been observed. The addition of inorganic particles in adhesive resins aims to decrease the degradation over time [17, 18] and, as a consequence, to reduce the composite structural defects that could lead to failures. The incorporation of fillers in adhesives can also lead to a hybrid layer with greater stability, thus contributing to the longevity of the restorative treatment [19].

✉ Vicente Castelo Branco Leitune
vicente.leitune@ufrgs.br

¹ Dental Materials Laboratory, School of Dentistry, Universidade Federal do Rio Grande do Sul, Rua Ramiro Barcelos, 2492 - Rio Branco, Porto Alegre, RS, Brazil

² Laboratory of Ceramic Materials, Universidade Federal do Rio Grande do Sul, Avenida Osvaldo Aranha 99, room 709 - Centro, Porto Alegre, RS, Brazil

Zirconia (ZrO_2) is a metallic oxide that is widely used in the biomedical field, especially in dentistry and other areas such as orthopedics: in fact, it is often utilized in hip prosthesis, because of its high compressive strength and biocompatibility [20, 21]. Among the oxides used in dentistry, zirconia presents the highest values of mechanical proprieties ever reported for any dental ceramic, bringing to this material considerable interest in dental field [22]. Zirconia is commonly stabilized in its tetragonal phase and applied as the main constituent of ceramic dental crowns, allowing the realization of posterior fixed partial dentures and the substantial reduction in the component's core thickness [20, 22]. The zirconia possesses a color similar to tooth with a high strength that is highly required in prosthetic dentistry [20, 23].

In the chemical industry, zirconia's monoclinic crystalline phase is widely used as a photocatalytic material [24, 25]. It has also shown to possess bioactive properties in both its monoclinic and tetragonal phases [21, 26]. In addition, particles of ZrO_2 were incorporated into composites that are currently marketed for dental restorative procedures, with the aim of improving its mechanical properties and reducing polymerization shrinkage [27]. Zirconia has also been incorporated as reinforcement for the repair strength of polymethyl methacrylate denture bases [28]. The increase in the volume ratio of the fillers incorporated into the matrix can add to the mechanical proprieties [29].

Some authors also suggest that the addition of zirconia nanoparticles seems to be a good method for producing radiopaque adhesives with increased microhardness [30]. The reduction of the particle size to nanoscale increases the surface area, leading to a higher reactivity [31]. As a result, chemical and biological activity can be enhanced [32]. However, to the best of our knowledge, there are no reports on the influence of zirconia nanoparticles in regard to the properties that are tested on this study on an adhesive resin. Therefore, the aim of this study was to develop an adhesive resin with the incorporation of zirconium dioxide in different concentrations, and evaluate the properties of the obtained composite.

Materials and methods

The experimental adhesives resins were formulated by mixing 50 wt.% bisphenol A glycerolate dimethacrylate (BisGMA), 25 wt.% triethylene glycol dimethacrylate (TEGDMA), and 25 wt.% 2-hydroxyethyl methacrylate (HEMA). As the photoinitiator system, camphoroquinone (CQ), ethyl 4-dimethylaminobenzoate (EDAB), and diphenyliodonium hexafluorophosphate (DPIHFP) at 1 mol% each were added to all groups. Also, butylated hydroxytoluene (BHT) was added at 0.01 wt.%. All of these materials were purchased by Aldrich Chemical Co. (St Louis, MO, USA). ZrO_2 was incorporated into the adhesive resin at concentrations of 0.5, 1, 4.8, and

9.1%, in weight. The control group was formulated without ZrO_2 incorporation. Zirconium dioxide was provided by Evonik (Essen, North Rhine-Westphalia, Germany). The ZrO_2 that was utilized in this study had no previous treatment.

The adhesive resin mixture was hand-mixed for 5 min, sonicated for 180 s and hand-mixed again for 5 min. To perform monomer photo-activation, a light-emitting diode unit (Ratii Cal, SDI Ltd., Bayswater, Victoria, Australia) was used. An irradiation value of 1200 mW/cm^2 was confirmed with a digital power meter (Ophir Optronics, North Andover, MA, USA).

Characterization of ZrO_2

X-ray diffraction

To identify the crystalline phases in the powder, a diffractometer (Philips X'Pert MPD Model) was used. The device operated at an acceleration voltage of 40 kV and an electrical current of 40 mA, using $CuK\alpha$ radiation. The scanning rate was $0.05^\circ/\text{min}$, and the time-step was 1 s.

Micro-Raman spectroscopy

The chemical groups of ZrO_2 compounds were identified by micro-Raman spectroscopy (SENTERRA model, Bruker Optics, Ettlingen, Germany). A laser with a 785-nm wavelength was used, with 100 mW of intensity, for 5 s and 2 co-additions. The range of analysis was $400\text{--}1200 \text{ cm}^{-1}$.

Surface area

The specific surface area of the ZrO_2 powder was determined through the Brunauer–Emmett–Teller (B.E.T) method, using a Quantachrome (NOVA1000 Autosorb Automated Gas Sorption System, Boynton Beach, FL, USA).

Degree of conversion

The degree of conversion (DC) for each of the experimental adhesive resins was evaluated using Fourier transform infrared (FTIR) spectroscopy with an infrared spectrometer (Vertex 70 model, Bruker Optics, Ettlingen, Baden-Württemberg, Germany) equipped with an attenuated total reflectance (ATR) device, and a horizontal diamond crystal with a mirror angle of 45° . Three samples ($n = 3$) of $3 \mu\text{L}$ were directly dispensed on to the diamond crystal and the measurement was performed before and immediately after the polymerization (light-activation for 20 s) [33]. The percentage of unreacted double carbon bonds ($\%C=C$) was determined by the ratio of the absorbance intensity between aliphatic double carbon bonds, considering its stretching vibration (peak height) at 1635 cm^{-1} , and using the symmetric ring stretching

at 1610 cm^{-1} from the polymerized and unpolymerized samples as an internal standard [3]. The DC was determined by subtracting the %C=C from 100%, as is described elsewhere [33].

Radiopacity

The radiopacity evaluation of each experimental adhesive was performed according to the International Organization of Standardization (ISO) 4049:2009 standards. Five samples ($n = 5$) of 10 mm (± 0.1 mm) in diameter and 1.0 mm (± 0.01 mm) in thickness were produced per group. The radiographic images were obtained using an X-ray source (Spectro 70X, Dabi Atlante, Ribeirão Preto, SP, Brazil) and a digital system with phosphorous plates (VistaScan; Durr Dental GmbH & Co. KG, Bietigheim-Bissingen, Alemanha) operating at 70 kV and 8 mA. Each X-ray image was taken with a focus-film distance of 400 mm and an exposure time of 0.4 s. A specimen from each group was placed on each plate for a total of five samples per plate. An aluminum step-wedge was exposed simultaneously with the specimens in all images. The thickness of the aluminum scale ranged from 0.5 to 5.0 mm in 0.5 mm increments. The images were saved in TIFF format and assessed using ImageJ (National Institutes of Health, Bethesda, Maryland, USA), by calculating the density of pixels in grayscale, applying the aluminum step-wedge for comparison.

Softening in solvent

To determine the softening in solvent, the specimens that were produced for radiopacity evaluation were used. Five specimens for each experimental adhesive ($n = 5$) were embedded in chemically activated acrylic resin and polished in a polisher machine (Model 3v, Arotec, Cotia, SP, Brazil), which used silicon carbide sandpaper with grain 600, 1200, and 2000 under constant irrigation. The specimens were submitted to a microhardness test, in which three indentations (15 g for 10 s), spaced 100 μm apart from each other were made on the surface of each specimen and assessed using an automatic microhardness tester (HMV-2 Shimadzu, Tokyo, Japan).

The initial Knoop hardness (KHN_1) was registered as the arithmetic average of five measurements. Once the KHN_1 results for each group were obtained, the specimens were immersed in absolute ethanol for a period of 4 h at $37\text{ }^\circ\text{C}$. After this period, the test was repeated in each specimen, and the post-conditioning hardness value was measured (KHN_2). The softening in solvent value was obtained by calculating the percentage difference between KHN_1 and KHN_2 .

Microtensile bond strength test

One hundred and twenty bovine lower incisors were stored in distilled water at $4\text{ }^\circ\text{C}$ for no more than 3 months. The teeth had the buccal enamel removed to expose the superficial dentin. A smear layer was produced by grinding the flat surface with a 600-grit silicon carbide (SiC) disc under constant irrigation. Prepared teeth were divided into five groups ($n = 24$). The exposed dentin were etched with 37% phosphoric acid for 15 s and rinsed off with distilled water for 30 s. A commercial primer (Primer, Scotchbond Multi-use, 3 M ESPE, St Paul, MN, USA) was applied for 20 s, and the solvent was evaporated with air spray for 5 s. Immediately after, adhesives were applied according to the experimental groups and photocured for 20 s using a LED curing light (Radii Cal, SDI, Australia). Two increments of composite resin (Z350, 3M ESPE, St Paul, MN, USA) were placed on the cured adhesive to cover the dentin surface completely. Both increments were photocured for 40 s each. The samples were stored in distilled water at $37\text{ }^\circ\text{C}$ for 24 h, and sectioned into sticks of 0.5 mm^2 of cross-sectional area. Twelve teeth were tested at 24 h, and the other 12 teeth sticks were stored in distilled water at $4\text{ }^\circ\text{C}$ for 1 year before testing. The sticks were fixed with a cyanoacrylate adhesive in a metallic device to be submitted to the microtensile bond strength test at a universal testing machine (EMIC DL-2000, Sao Jose dos Pinhais, PR, Brazil) with a crosshead speed of 1 mm/min. The values of bond strength were calculated in MPa and the tooth was considered to be the sample unit.

Interface characterization by micro-Raman

The interface between adhesive and underlying dentin was analyzed by micro-Raman vibrational microscopy. The parameters were asserted to a 100 mW diode laser with a 785 nm wavelength and a spectral resolution of $\sim 3.5\text{ cm}^{-1}$ at a Raman microscope (SENTERRA, Bruker Optics, Ettlingen, Germany). Sticks produced for microtensile evaluation were used. Dimensional mapping was performed over a 100- μm line across the adhesive–dentin interface at 1- μm intervals using a XYZ stage. Post-processing was performed in Opus 6.5 software (Bruker Optics) and consisted of analysis with modeling, which distinguished spectral components of the adhesive and dentin. One correspondent peak of each substance was used for integration: phosphate at 960 cm^{-1} [34], methacrylate at 1610 cm^{-1} [3], and zirconia at 476 cm^{-1} [35].

Mineral deposition

Restorations were made on bovine dentin as already described for microtensile bond strength, and interfaces were subsequently produced by sectioning perpendicular to dentin-

adhesive interface, with a diamond disc at high speed under constant irrigation. The mineral deposition was analyzed by micro-Raman spectroscopy (SENTERRA Raman Microscope, Bruker Optics, Ettlingen, Germany), using the same parameters described above. Two-dimensional mappings were performed by group, over a $50 \times 20\text{-}\mu\text{m}$ predetermined area, at $1\text{-}\mu\text{m}$ intervals. The analysis was performed 24 h after photocuring, and then, immersed in 20 mL of simulated body fluid (SBF) [36], and re-evaluated on the same area of the sample after 14 days of immersion. The previously known phosphate peak (960 cm^{-1}) [34] was used for integration and evaluation of mineral deposition at the interface area.

Statistical analysis

The normality of the data was evaluated using the Shapiro-Wilk test. Statistical analysis was performed using one-way ANOVA (ZrO_2 concentration) for radiopacity, softening in solvent and DC. For the analysis of softening in solvent, a paired Student's *t* test (KHN_1 and KHN_2) was used. The data from μTBS were analyzed through two-way ANOVA (ZrO_2 concentration and time). Tukey's post hoc test was used for multiple comparisons in all obtained data. All tests were performed at a 0.05 level of significance.

Results

The X-ray diffraction spectrum of the analyzed sample is shown in Fig. 1. It was possible to identify two polymorphic phases of ZrO_2 . The combined JCPDS pattern of baddeleyite or primitive monoclinic ZrO_2 (24–1165) and the ICSD pattern of tetragonal ZrO_2 (068781) match with the observed XRD peaks. The specific value of the ZrO_2 surface particles shown by B.E.T. is $37.41\text{ m}^2/\text{g}$. The Raman spectra are presented in Fig. 2, revealing the typical chemical groups of ZrO_2 compounds, with the appearance of the 476 cm^{-1} peak [35].

The DC values are presented in Table 1. All groups showed DC higher than 70% and ranged from 71.7 (± 0.3) in the control group to 76.7 (± 0.3) at 1% ZrO_2 incorporation. Only the group with addition of 1% ZrO_2 significantly increased DC compared to the control group ($P < 0.05$).

The values for Knoop hardness before and after immersion in the solvent and the degradation percentages are shown in Table 1. The group with 4.8% ZrO_2 presented higher initial mean values of Knoop hardness (KHN_1) than the control group ($P < 0.05$). After immersion in solvent, all groups presented reduction in hardness values (KHN_2). The percentage of hardness reduction was higher as an increased the concentration of ZrO_2 was incorporated; however, the groups with addition of 0.5 and 1% ZrO_2 experienced no difference compared to the control group ($P < 0.05$).

The radiopacity values of the dental adhesive resins are presented in Fig. 3. There was no difference between groups with ZrO_2 incorporation and the control group ($P < 0.05$).

The mean and standard deviation values of microtensile bond strength (μTBS) after 24 h and 1 year of aging are shown in Table 2. There was no statistical difference between groups in 24 h or in 1 year, except for the 9.1% concentration that presented a significant reduction in μTBS after 1 year aging. In 24 h test, the values ranged from 45.23 to 55.81 MPa. After 1 year the values ranged from 30.92 to 52.94 MPa.

A representative image from the interface characterization by micro-Raman spectroscopy is shown in Fig. 4a. The colored scale located on the right represents the amount, through the assessed area, of the elements that are the corresponding peaks used for integration. It was possible to observe the presence of adhesive across the hybrid layer and the penetration of nanostructured zirconia at almost the same extension of dentin demineralization. On Fig. 4b, the Raman spectra, for phosphate (960 cm^{-1}) and methacrylate (1610 cm^{-1}) peaks are represented for the principal components (D) dentin, (A) adhesive, (HL), hybrid layer, and (R) composite resin. Representative images of interfaces evaluated by micro-Raman spectroscopy for mineral deposition at the baseline (24 h) and 14 days after immersion in SBF are shown in Fig. 4c. After 14 days, the groups with the 4.8 and 9.1% addition of ZrO_2 promoted mineral deposition compared to the control group.

Discussion

In this study, adhesive resins were formulated with the incorporation of zirconia nanofillers. The addition of 1 wt.% ZrO_2 resulted in a significant increase in the DC without compromising the other physicochemical characteristics. The DC of the experimental adhesive resins presented values higher than 70% for all groups. The particles of the oxide presented two crystalline phases (monoclinic and tetragonal), a favorable superficial area, which allows for great reactivity and a penetration into the hybrid layer. Moreover, the addition of 4.8 and 9.1% of ZrO_2 promoted mineral deposition over the dentin-adhesive interface. These characteristics indicate that zirconium dioxide may be a promising filler in dental resin adhesives.

A dental adhesive should ideally present enough radiopacity to allow discrimination between dental tissues and the composite material, thus enabling the differential diagnosis of secondary caries [15, 37, 38]. This characteristic is mainly related to the atomic number (*Z*) and material thickness [39]. Although zirconium ($Z = 40$) presents considerable radiopacity when composing dental ceramic systems, the minimum application thickness of 2 mm is always required for enough radiopacity [20], which is not possible for the thinner

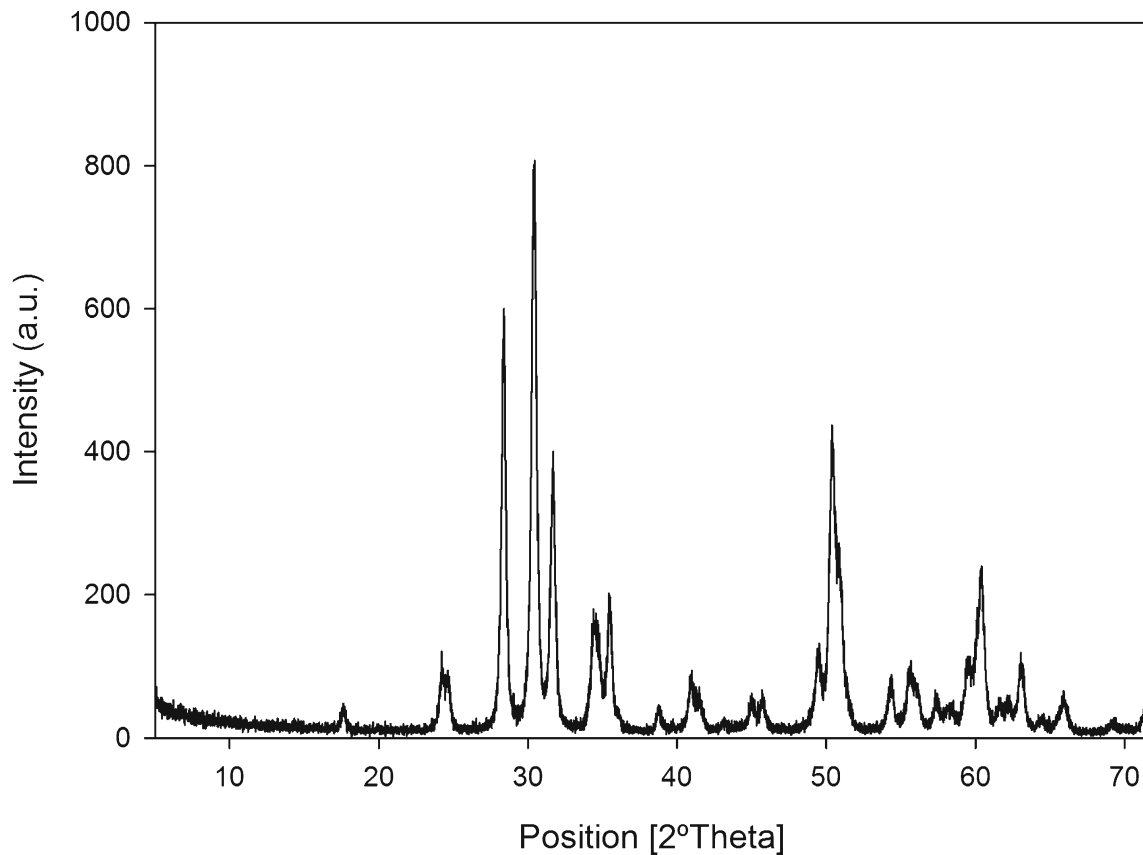


Fig. 1 XRD pattern of the zirconium dioxide powder

thickness of the adhesive resin layer. Current commercial composites containing ZrO_2 are shown to be sufficiently radiopaque and present up to 80 wt.% of the filler content [40], which is a higher amount than those used in this study. However, the amount of filler to be incorporated in adhesives is limited considering that low viscosity is required. ISO 4049 recommends that the minimum value for radiopacity should be 1 mmAl and even though the addition of ZrO_2 was unable to increase the radiopacity of experimental adhesive resins, the values obtained in this study are comparable with most adhesives currently available on the market [15]. Regarding this, there is the possibility of associating to the experimental

adhesives another material with higher radiopacity [41] while conserving the advantageous characteristics of zirconia at lower concentrations.

The DC is shown as the percentage of consumption of aliphatic bonds during the polymerization and is not only associated with increased mechanical properties, but also with the polymer stability [19, 42]. A low DC values can lead to a more soluble polymer, consequently enhancing its degradation since it contains a higher amount of unreacted monomers in the polymeric matrix [19, 33]. Using the same methods of measurement and the conventional irradiation conditions of this study, a DC between 55 and 75% is acceptable for

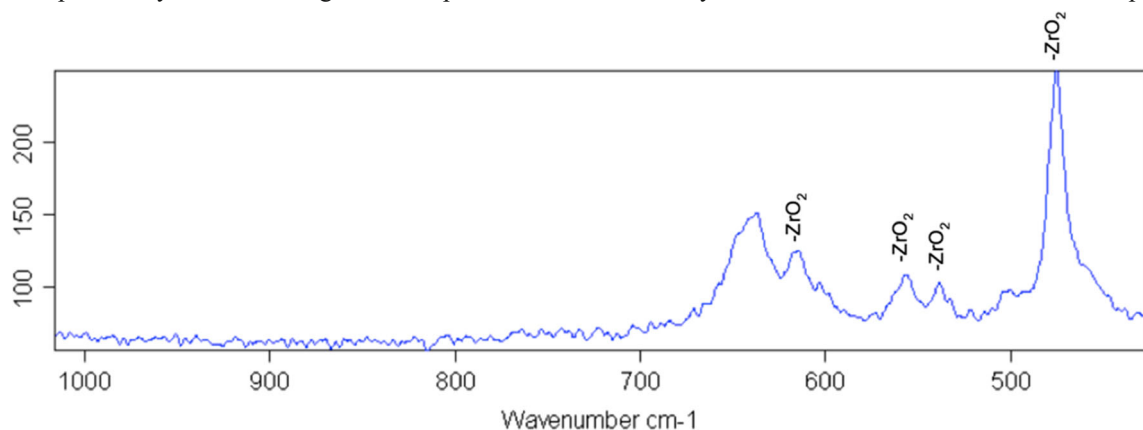


Fig. 2 Micro-Raman spectrum of the zirconium dioxide powder

Table 1 Mean and standard deviation values of degree of conversion (DC), hardness of the adhesive before (KHN₁) and after immersion in solvent (KHN₂), and the variation of hardness values ($\Delta\%$)

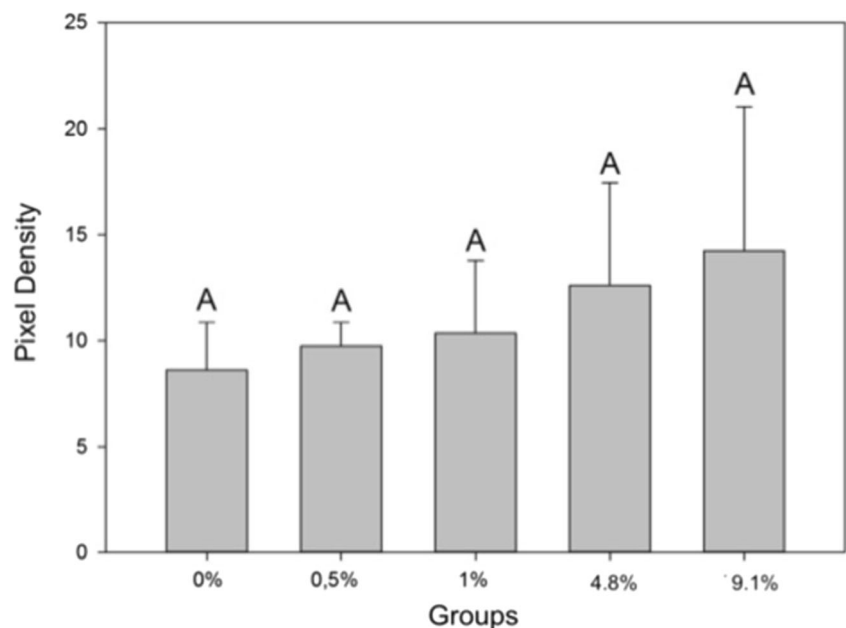
Groups (%)	DC	KHN ₁	KHN ₂	$\Delta\%$
0	71.7(0.3) ^B	21.4 (1.0) ^{BCa}	16.8 (2.0) ^b	-21.3 (7.0) ^A
0.5	74.0(0.4) ^{AB}	21.4 (1.8) ^{BCa}	17.6 (1.3) ^b	-17.1 (9.1) ^A
1	76.7(0.3) ^A	20.6 (2.7) ^{Ca}	13.8 (3.6) ^b	-33.2 (13.3) ^{AB}
4.8	73.0(3.1) ^{AB}	26.2 (2.0) ^{Aa}	15.4 (1.4) ^b	-40.7 (8.1) ^B
9.1	72.0(1.1) ^B	24.6 (1.5) ^{ABa}	13.1 (1.9) ^b	-46.3 (10.1) ^B

Different capital letters indicate statistically significant difference in the same column ($P < 0.05$)

Different small letters indicate statistically significant difference in the line ($P < 0.05$)

adhesive resins [43], and all groups showed DC higher than 55%. The increase of monomer conversion may be related to changes in the kinetics ruled by the increase in filler concentration, as they promote the homogenization of the spatially sites for monomer reaction [44].

Zirconia already demonstrated photocatalytic activity in previous studies [24, 25], with great light absorption band close to those irradiated by LED [25]. The ZrO₂ particles, whose refractive index can be as high as 2.1–2.3 [45, 46], could adversely affect the DC due to its optical scattering properties responsible for opacity. However, it was observed that the addition of zirconia showed no difference from control the group, except in the group with 1% ZrO₂, which significantly increased the DC ($P < 0.05$). The increase in DC could be related to the small size of the particles, with diameters below one-tenth of the wavelength of visible light (400–800 nm) and typically <25 nm, which can avoid Rayleigh scattering, grant better particle reactivity and allow

Fig. 3 Mean and standard deviation values for radiopacity of adhesive resin. Equal capital letters indicate no statistical difference ($p < 0.05$)**Table 2** Mean and standard deviation values of the μ TBS test in 24 h and after 1 year of water aging

Groups (%)	μ TBS 24 h	μ TBS 1 year
0	55.81 (21.41) ^{Aa}	41.72 (12.96) ^{Aa}
0.5	52.23 (18.00) ^{Aa}	52.94 (24.23) ^{Aa}
1	55.57 (18.73) ^{Aa}	45.80 (9.21) ^{Aa}
4.8	45.23 (17.97) ^{Aa}	42.04 (11.35) ^{Aa}
9.1	52.25 (9.42) ^{Aa}	30.92 (13.29) ^{Ab}

Different capital letters indicate statistically significant difference in the same column ($P < 0.05$)

Different small letters indicate statistically significant difference in the line ($P < 0.05$)

incorporation into a transparent polymer matrix [46]. Nevertheless, groups with higher incorporation of ZrO₂ (4.8 and 9.1%) resulted in a significant increase in the opacity of the polymer, which may explain the lower DC values in these groups.

When exposed to a solvent, the filled adhesive resins behavior can be correlated with its stability in the oral environment [2, 19], and its ability to withstand hydrolytic degradation [1]. Degradation occurs due to the solvent's penetration and its diffusion into the composite structure, leading to an elution of its components [19]. Polymers with higher amounts of cross-linking are less prone to degradation considering the limited solvent diffusion [19]. Also, it is important to mention that the ZrO₂ particles were not silanized in this study because the silane could not bond with the filler (zirconia), as there is no chemical interaction between these two materials. When the silane is not bonded with the inorganic filler and/or to the organic matrix, the hydrolytic stability is compromised, leading to bond degradation over time in the oral environment

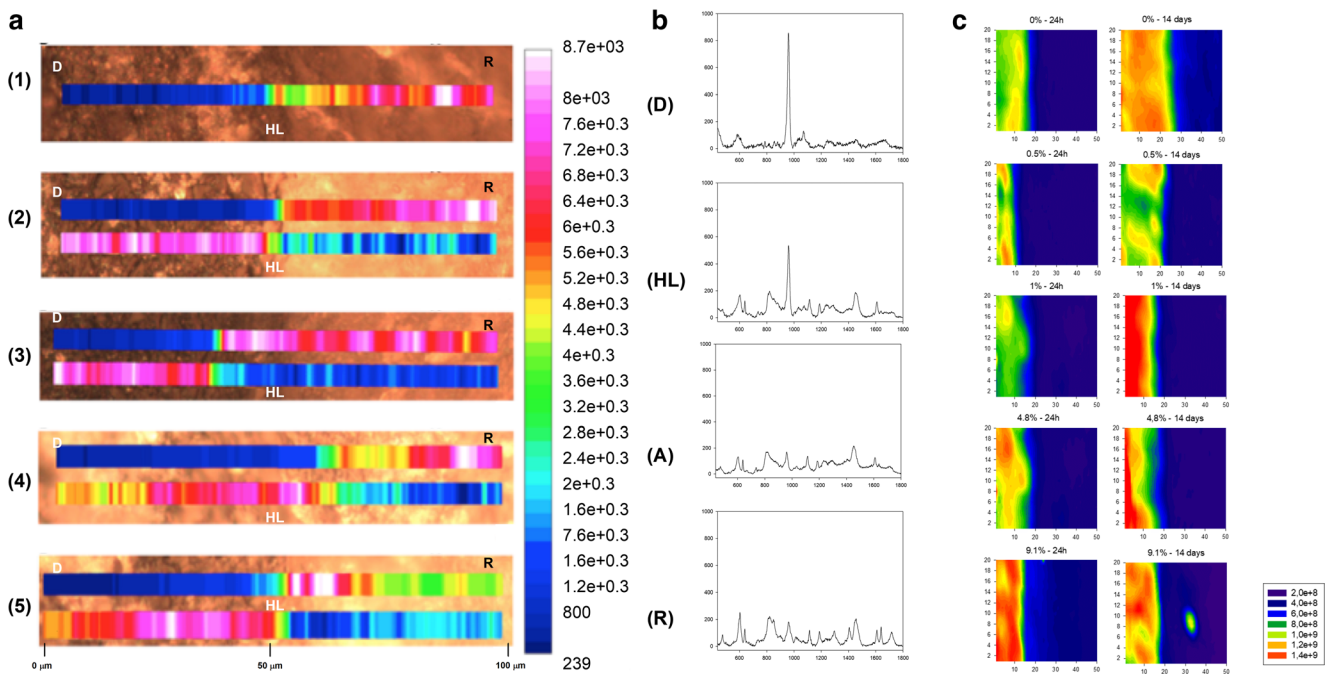


Fig. 4 Experimental Adhesive resin with the addition of (1) 0% ZrO₂, (2) 0.5% ZrO₂, (3) 1% ZrO₂, (4) 4.8% ZrO₂, and (5) 9.1% ZrO₂. **a** Dentin-adhesive interfaces characterization and representative color scale (right located), in which, composite resin (R), dentin (D) and the hybrid layer (HL) are represented inside images. The adhesive without ZrO₂ was integrated by methacrylate peak (1610 cm⁻¹) at (1) line and, for (2), (3),

(4), and (5) lines; interface was integrated by zirconia peak (476 cm⁻¹) above and phosphate peak (960 cm⁻¹) below. **b** Raman spectra, for phosphate (960 cm⁻¹) and methacrylate (1610 cm⁻¹) peaks, of principal components (D) dentin, (A) adhesive, (HL) hybrid layer, and (R) composite resin. **c** Micro-Raman map of the phosphate peak (961 cm⁻¹) intensities at the dentin bonded interface at baseline and after 14 days immersed in SBF

[47]. The immersion of the specimens in the SBF medium leads to an adsorption of OH⁻ ions and formation of hydroxide bonds with zirconia, which assist in the subsequent formation of the HAp phase through deposition by Ca²⁺ ions [21]. Therefore, the silanization of the particles could negatively affect the ion release, due to the hydrophobic silane coating on the particles, thus retarding the access of water to the particles and slowing their dissolution [48]. In our study, the results of the 4.8% ZrO₂ group presented higher initial mean values of Knoop hardness than the control group (*P* < 0.05), and after immersion in the solvent, all groups presented reduction in hardness values. With the polymeric network degradation, the filler particles may leach from the material [49], therefore, the use of biocompatible fillers, such as zirconium dioxide [20, 21], could prevent cytotoxicity effects.

Another study which incorporated zirconia in a commercial adhesive only observed the enhancement in Knoop hardness in groups with at least 24.8% of filler incorporation [30]. The increase of particle content suggests that the surrounding matrix complies less, and it could explain why the increase on microhardness cannot always be detected in small concentrations [50]. In the group with 9.1% ZrO₂, even with the highest amount of incorporation, the increase in hardness was probably not significant because the filler was not distributed in an homogenic arrangement of particles in the matrix. During the Knoop hardness test, the zirconium oxide particles are pressed into the softer polymeric matrix, alternately than being

plastically deformed under the tested load; due to this, they may not display their true intrinsic microhardness [50].

In the present study, Raman spectra showed the presence of adhesives across the hybrid layer. It was also possible to observe the penetration of nanostructured zirconia at almost the same extension of dentin demineralization, allowing its interaction with dentin tissue. The addition of the filler to the hybrid layer could improve its mechanical properties and enhance its stability, and once zirconia is known to be bioactive when assuming a tetragonal and/or monoclinic structure [21], this could improve the bond strength durability by forming Zr-OH groups when in contact with the tubular fluid. These groups could promote effective apatite nucleation and its precipitation onto the interface [51]. The verification of the bioactivity of an artificial material can be made by examining the formation of apatite on its surface in simulated body fluid [36].

Raman spectrum indicated the mineral deposition over the hybrid layer, as the phosphate peak (960 cm⁻¹) appeared on the spectra, thus indicating a mineral precipitation over the analyzed area [52, 53]. The Raman spectroscopy technique is considered a powerful method to analyze the resin–dentin interface and the mineral content distribution by some authors, as it shows the chemical changes along the analyzed area [54, 55]. The interface evaluation for mineral deposition showed higher results for the groups with a greater amount of ZrO₂. All specimens presented an increase in mineral content over

time. The remineralization process is achieved through the mineral deposition over the remnant seed crystallites at the basal part of the collagen matrix, which can act as centers for heterogeneous nucleation [56, 57]. The deposition of mineral via ion-by-ion release (epitaxial growth) is regarded as a top-down approach according to the classical crystallization theory [57]. The mineral deposition showed by the 4.8 wt.% group was also confirmed by an increasing in Knoop hardness, as the ongoing restoration of mechanical properties is directly related to the precipitation of minerals [58].

The bond strength was immediately evaluated by the microtensile test and after aging in distilled water for 1 year. A difference was found after aging for 9.1% incorporation, which significantly reduced the μ TBS, even with the presence of zirconia in the hybrid layer and the promotion of mineral deposition for this group. The overall degradation could not be prevented, but it must be considered that specimens were stored in distilled water, which could have increased the particles' susceptibility to aging and damaged the uniform mineral deposition on the dentin-adhesive interface. To overcome this issue, a resin matrix with the addition of phosphonated monomers that chemically interact with ZrO_2 groups could be formulated in future studies [59].

Zirconia nanoparticles were incorporated at different concentrations in a commercial adhesive by one study; however, there was a significant increase in the immediate bond strength to dentin, with no difference between the concentrations [26]. In contrast to this study, the particles used were stabilized by yttria (Y_2O_3), and it may have reduced the martensitic transformation ($t \rightarrow m$) presented by zirconia particles [22, 60–62]. The martensitic transformation leads to an alteration of its phase integrity and increases its susceptibility to aging [28, 63]. This transformation could have influenced the bond strength in this study as it reduces the resistance of ZrO_2 to crack propagation. Regarding the results discussed, zirconium dioxide may be an alternative filler for polymer-based biomaterials at lower concentrations.

Conclusion

In the present study, adhesive resins with ZrO_2 incorporation were formulated. The incorporation of 1 wt.% ZrO_2 significantly increased the DC, promoted the ability to infiltrate through the hybrid layer, and it could be a promising filler for adhesive development.

Acknowledgements The authors gratefully acknowledge CNPq (Conselho Nacional de Desenvolvimento Científico e Tecnológico) for the scholarship.

Funding The work was supported by CNPq (Conselho Nacional de Desenvolvimento Científico e Tecnológico).

Compliance with ethical standards

Conflict of interest The authors declare that they have no conflict of interest.

Ethical approval This article does not contain any studies with human participants or animals performed by any of the authors.

References

1. De Munck J, Van Landuyt K, Peumans M, Poitevin A, Lambrechts P, Braem M, van Meerbeek B (2005) A critical review of the durability of adhesion to tooth tissue: methods and results. *J Dent Res* 84(2):118–132. <https://doi.org/10.1177/154405910508400204>
2. Van Landuyt KL, Snaauwaert J, De Munck J, Peumans M, Yoshida Y, Poitevin A, Coutinho E, Suzuki K, Lambrechts P, Van Meerbeek B (2007) Systematic review of the chemical composition of contemporary dental adhesives. *Biomaterials* 28(26):3757–3785. <https://doi.org/10.1016/j.biomaterials.2007.04.044>
3. Collares FM, Ogliaari FA, Zanchi CH, Petzhold CL, Piva E, Samuel SM (2011) Influence of 2-hydroxyethyl methacrylate concentration on polymer network of adhesive resin. *J Adhes Dent* 13(2):125–129. <https://doi.org/10.3290/j.jad.a18781>
4. Leitune VC, Collares FM, Trommer RM, Andrioli DG, Bergmann CP, Samuel SMW (2013) Niobium pentoxide as a novel filler for dental adhesive resin. *J Dent* 41(2):106–113. <https://doi.org/10.1016/j.jdent.2012.04.022>
5. Sano H, Takatsu T, Ciucchi B, Homer JA, Matthews WG, Pashley DH (1995) Nanoleakage: leakage within the hybrid layer. *Oper Dent* 20(1):18–25
6. Sano H, Yoshiyama M, Ebisu S, Burrow MF, Takatsu T, Ciucchi B, Carvalho R, Pashley DH (1995) Comparative SEM and TEM observations of nanoleakage within the hybrid layer. *Oper Dent* 20(4):160–167
7. Zhang SC, Kern M (2009) The role of host-derived dentinal matrix metalloproteinases in reducing dentin bonding of resin adhesives. *Int J Oral Sci* 1(4):163–176. <https://doi.org/10.4248/IJOS.09044>
8. De Munck J, Mine A, Van den Steen PE, Van Landuyt KL, Poitevin A, Opdenakker G, Van Meerbeek B (2010) Enzymatic degradation of adhesive-dentin interfaces produced by mild self-etch adhesives. *Eur J Oral Sci* 118(5):494–501. <https://doi.org/10.1111/j.1600-0722.2010.00758.x>
9. Nikaido T, Nurrohman H, Takagaki T, Sadr A, Ichinose S, Tagami J (2015) Nanoleakage in hybrid layer and acid-base resistant zone at the adhesive/dentin interface. *Microsc Microanal* 21(05):1271–1277. <https://doi.org/10.1017/S1431927615015068>
10. Kondo Y, Takagaki T, Okuda M, Ikeda M, Kadoma Y, Yamauchi J, Okada K, Sadr A, Nikaido T, Tagami J (2010) Effect of PMMA filler particles addition on the physical properties of resin composite. *Dent Mater J* 29(5):596–601. <https://doi.org/10.4012/dmj.2009-141>
11. Fujita K, Ikemi T, Nishiyama N (2011) Effects of particle size of silica filler on polymerization conversion in a light-curing resin composite. *Dent Mater* 27(11):1079–1085. <https://doi.org/10.1016/j.dental.2011.07.010>
12. Skovgaard M, Ahniyaz A, Sørensen BF, Almdal K, van Lelieveld A (2010) Effect of microscale shear stresses on the martensitic phase transformation of nanocrystalline tetragonal zirconia powders. *J Eur Ceram Soc* 30(13):2749–2755. <https://doi.org/10.1016/j.jeurceramsoc.2010.05.025>
13. Coldea A, Swain MV, Thiel N (2013) Mechanical properties of polymer-infiltrated-ceramic-network materials. *Dent Mater* 29(4):419–426. <https://doi.org/10.1016/j.dental.2013.01.002>

14. Leitune VCB, Collares FM, Trommer RM, Andrioli DG, Bergmann CP, Samuel SMW (2013) The addition of nanostructured hydroxyapatite to an experimental adhesive resin. *J Dent* 41(4):321–327. <https://doi.org/10.1016/j.jdent.2013.01.001>
15. Schulz H, Schimmoeller B, Pratsinis SE, Salz U, Bock T (2008) Radiopaque dental adhesives: dispersion of flame-made Ta₂O₅/SiO₂ nanoparticles in methacrylic matrices. *J Dent* 36(8):579–587. <https://doi.org/10.1016/j.jdent.2008.04.010>
16. Sun J, Petersen EJ, Watson SS, Sims CM, Kassman A, Frukhtbeyn S, Skrtic D, Ok MT, Jacobs DL, Reipa V, Ye Q, Nelson BC (2017) Biophysical characterization of functionalized titania nanoparticles and their application in dental adhesives. *Acta Biomater* 53:585–597. <https://doi.org/10.1016/j.actbio.2017.01.084>
17. Ragosta GAM, Musto P (2005) Epoxy-silica particulate nanocomposites: chemical interactions, reinforcement and fracture toughness. *Polymer* 46(23):10506–10516. <https://doi.org/10.1016/j.polymer.2005.08.028>
18. Garcia IM, Leitune VC, Kist TL, Takimi A, Samuel SM, Collares FM (2016) Quantum dots as nonagglomerated nanofillers for adhesive resins. *J Dent Res* 95(12):1401–1407. <https://doi.org/10.1177/0022034516656838>
19. Ferracane JL (2006) Hygroscopic and hydrolytic effects in dental polymer networks. *Dent Mater* 22(3):211–222. <https://doi.org/10.1016/j.dental.2005.05.005>
20. Manicone PF, Rossi Iommetti P, Raffaelli L (2007) An overview of zirconia ceramics: basic properties and clinical applications. *J Dent* 35(11):819–826. <https://doi.org/10.1016/j.jdent.2007.07.008>
21. Sarkar D, Swain SK, Adhikari S, Reddy BS, Maiti HS (2013) Synthesis, mechanical properties and bioactivity of nanostructured zirconia. *Mater Sci Eng C Mater Biol Appl* 33(6):3413–3417. <https://doi.org/10.1016/j.msec.2013.04.036>
22. Denry I, Kelly JR (2008) State of the art of zirconia for dental applications. *Dent Mater* 24(3):299–307. <https://doi.org/10.1016/j.dental.2007.05.007>
23. Höland WSM, Watzke R, Peschke A, Kappert H (2008) Ceramics as biomaterials for dental restoration. *Expert Rev Med Devices* 5(6):729–745. <https://doi.org/10.1586/17434440.5.6.729>
24. Karunakaran CSS (2005) Photocatalysis with ZrO₂: oxidation of aniline. *J Mol Catal A Chem* 233(1-2):4–8. <https://doi.org/10.1016/j.molcata.2005.01.038>
25. Mishra T, Hait J, Aman N, Jana RK, Chakravarty S (2007) Effect of UV and visible light on photocatalytic reduction of lead and cadmium over titania based binary oxide materials. *J Colloid Interface Sci* 316(1):80–84. <https://doi.org/10.1016/j.jcis.2007.08.037>
26. Lohbauer U, Wagner A, Belli R, Stoetzel C, Hilpert A, Kurland HD, Grabow J, Muller FA (2010) Zirconia nanoparticles prepared by laser vaporization as fillers for dental adhesives. *Acta Biomater* 6(12):4539–4546. <https://doi.org/10.1016/j.actbio.2010.07.002>
27. Skovgaard M, Almdal K, Sørensen BF, Linderth S, van Lelieveld A (2011) Shrinkage reduction of dental composites by addition of expandable zirconia filler. *J Compos Mater* 46(26):5–2822. <https://doi.org/10.1177/0021998311401936>
28. Deville S, Chevalier J, Gremillard L (2006) Influence of surface finish and residual stresses on the ageing sensitivity of biomedical grade zirconia. *Biomaterials* 27(10):2186–2192. <https://doi.org/10.1016/j.biomaterials.2005.11.021>
29. Allaker RPRG (2008) Potential impact of nanotechnology on the control of infectious diseases. *Trans R Soc Trop Med Hyg* 102(1):1–2. <https://doi.org/10.1016/j.trstmh.2007.07.003>
30. Martins GC, Meier MM, Loguercio AD, Cecchin F, Gomes OMM, Reis A (2013) Effects of zirconia nanoparticles addition to experimental adhesives on radiopacity and microhardness. *Braz J Oral Sci* 12(4):319–322. <https://doi.org/10.1590/S1677-32252013000400008>
31. Lanone S, Boczkowski J (2006) Biomedical applications and potential health risks of nanomaterials: molecular mechanisms. *Curr Mol Med* 6(6):651–663. <https://doi.org/10.2174/156652406778195026>
32. Raghupathi KR, Koodali RT, Manna AC (2011) Size-dependent bacterial growth inhibition and mechanism of antibacterial activity of zinc oxide nanoparticles. *Langmuir* 27(7):4020–4028. <https://doi.org/10.1021/la104825u>
33. Collares FM, Portella FF, Leitune VC, Samuel SM (2014) Discrepancies in degree of conversion measurements by FTIR. *Braz Oral Res* 28(6):9–15. <https://doi.org/10.1590/S1806-83242013000600002>
34. Miyazaki M, Sato H, Onose H, Moore BK, Platt JA (2003) Analysis of the enamel/adhesive resin interface with laser Raman microscopy. *Oper Dent* 28(2):136–142
35. Miciukiewicz J, Mang T, Knözinger H (1995) Raman spectroscopy characterization of molybdena supported on titania-zirconia mixed oxide. *Appl Catal A Gen* 122(2):151–159. [https://doi.org/10.1016/0926-860X\(94\)00236-3](https://doi.org/10.1016/0926-860X(94)00236-3)
36. Kokubo T, Takadama H (2006) How useful is SBF in predicting in vivo bone bioactivity? *Biomaterials* 27(15):2907–2915. <https://doi.org/10.1016/j.biomaterials.2006.01.017>
37. Collares FM, Ogliaeri FA, Lima GS, Fontanella VR, Piva E, Samuel SM (2010) Ytterbium trifluoride as a radiopaque agent for dental cements. *Int Endod J* 43(9):792–797. <https://doi.org/10.1111/j.1365-2591.2010.01746.x>
38. de Moraes Porto IC, Honorio NC, Amorim DA, de Melo Franco AV, Penteado LA, Parolia A (2014) Comparative radiopacity of six current adhesive systems. *J Conserv Dent* 17(1):65–69. <https://doi.org/10.4103/0972-0707.124151>
39. Bowen RL, Cleek GW (1972) A new series of x-ray-opaque reinforcing fillers for composite materials. *J Dent Res* 51(1):177–182. <https://doi.org/10.1177/00220345720510011301>
40. Reges RVCF, Adabo GL, Cruz CAS, Sobrinho LC (2002) Análise quantitativa do conteúdo de carga inorgânica das resinas compostas/Quantitative analysis of the content of load inorganic of the composite resin. *Braz Dent Sci* 5(2):18–22. <https://doi.org/10.14295/bds.2002.v5i2.153>
41. Neftali C, Thiago O, Evandro P, Fernanda L, Giana L, Marcelo M, Cristiane R, Fabrício O (2012) YbF₃/SiO₂ fillers as radiopacifiers in a dental adhesive resin. *Nano-Micro Lett* 4:189–196. <https://doi.org/10.3786/nml.v4i3.p189-196>
42. Ferracane JL (1985) Correlation between hardness and degree of conversion during the setting reaction of unfilled dental restorative resins. *Dent Mater* 1(1):11–14. [https://doi.org/10.1016/s0109-5641\(85\)80058-0](https://doi.org/10.1016/s0109-5641(85)80058-0)
43. Stansbury JW, Dickens SH (2001) Determination of double bond conversion in dental resins by near infrared spectroscopy. *Dent Mater* 17(1):71–79. [https://doi.org/10.1016/S0109-5641\(00\)00062-2](https://doi.org/10.1016/S0109-5641(00)00062-2)
44. Belli R, Kreppel S, Petschelt A, Hornberger H, Boccaccini AR, Lohbauer U (2014) Strengthening of dental adhesives via particle reinforcement. *J Mech Behav Biomed Mater* 37:100–108. <https://doi.org/10.1016/j.jmbbm.2014.05.007>
45. Luo K, Zhou S, Wu L (2009) High refractive index and good mechanical property UV-cured hybrid films containing zirconia nanoparticles. *Thin Solid Films* 517(21):5974–5980. <https://doi.org/10.1016/j.tsf.2009.03.162>
46. Nakayama N, Hayashi T (2007) Preparation and characterization of TiO₂-ZrO₂ and thiol-acrylate resin nanocomposites with high refractive index via UV-induced crosslinking polymerization. *Compos A: Appl Sci Manuf* 38(9):1996–2004. <https://doi.org/10.1016/j.compositesa.2007.05.005>
47. Lung CY, Matinlinna JP (2012) Aspects of silane coupling agents and surface conditioning in dentistry: an overview. *Dent Mater* 28(5):467–477. <https://doi.org/10.1016/j.dental.2012.02.009>
48. Xu HH, Weir MD, Sun L (2007) Nanocomposites with Ca and PO₄ release: effects of reinforcement, dicalcium phosphate particle size

- and silanization. *Dent Mater* 23(12):1482–1491. <https://doi.org/10.1016/j.dental.2007.01.002>
49. Soderholm KJ, Yang MC, Garcea I (2000) Filler particle leachability of experimental dental composites. *Eur J Oral Sci* 108(6):555–560. <https://doi.org/10.1034/j.1600-0722.2000.00919.x>
 50. Krumova M, Klingshirn C, Hauptert F, Friedrich K (2001) Microhardness studies on functionally graded polymer composites. *Compos Sci Technol* 61(4):557–563. [https://doi.org/10.1016/S0266-3538\(00\)00228-1](https://doi.org/10.1016/S0266-3538(00)00228-1)
 51. Uchida M, Kim H-M, Kokubo T, Miyaji F, Nakamura T (2001) Bonelike apatite formation induced on zirconia gel in a simulated body fluid and its modified solutions. *J Am Ceram Soc* 84(9):2041–2044. <https://doi.org/10.1111/j.1151-2916.2001.tb00955.x>
 52. Osorio R, Osorio E, Medina-Castillo AL, Toledano M (2014) Polymer nanocarriers for dentin adhesion. *J Dent Res* 93(12):1258–1263. <https://doi.org/10.1177/0022034514551608>
 53. Portella FF, Collares FM, Dos Santos LA, dos Santos BP, Camassola M, Leitune VC, Samuel SM (2015) Glycerol salicylate-based containing alpha-tricalcium phosphate as a bioactive root canal sealer. *J Biomed Mater Res B Appl Biomater* 103(8):1663–1669. <https://doi.org/10.1002/jbm.b.33326>
 54. Toledano M, Aguilera FS, Cabello I, Osorio R (2014) Remineralization of mechanical loaded resin-dentin interface: a transitional and synchronized multistep process. *Biomech Model Mechanobiol* 13(6):1289–1302. <https://doi.org/10.1007/s10237-014-0573-9>
 55. Sauro S, Osorio R, Watson TF, Toledano M (2015) Influence of phosphoproteins' biomimetic analogs on remineralization of mineral-depleted resin-dentin interfaces created with ion-releasing resin-based systems. *Dent Mater* 31(7):759–777. <https://doi.org/10.1016/j.dental.2015.03.013>
 56. Kim J, Arola DD, Gu L, Kim YK, Mai S, Liu Y, Pashley DH, Tay FR (2010) Functional biomimetic analogs help remineralize apatite-depleted demineralized resin-infiltrated dentin via a bottom-up approach. *Acta Biomater* 6(7):2740–2750. <https://doi.org/10.1016/j.actbio.2009.12.052>
 57. Dai L, Liu Y, Salameh Z, Khan S, Mao J, Pashley DH, Tay FR (2011) Can caries-affected dentin be completely remineralized by guided tissue remineralization? *Dent Hypotheses* 2(2):74–82. <https://doi.org/10.5436/j.dehy.2010.1.00011>
 58. Burwell AK, Thula-Mata T, Gower LB, Habelitz S, Kurylo M, Ho SP, Chien YC, Cheng J, Cheng NF, Gansky SA, Marshall SJ, Marshall GW (2012) Functional remineralization of dentin lesions using polymer-induced liquid-precursor process. *PLoS One* 7(6):e38852. <https://doi.org/10.1371/journal.pone.0038852>
 59. Nagaoka N, Yoshihara K, Feitosa VP, Tamada Y, Irie M, Yoshida Y, van Meerbeek B, Hayakawa S (2017) Chemical interaction mechanism of 10-MDP with zirconia. *Sci Rep* 7:45563–45569. <https://doi.org/10.1038/srep45563>
 60. Kelly PM, Francis Rose LR (2002) The martensitic transformation in ceramics — its role in transformation toughening. *Prog Mater Sci* 47(5):463–557. [https://doi.org/10.1016/S0079-6425\(00\)00005-0](https://doi.org/10.1016/S0079-6425(00)00005-0)
 61. Garvie RC, Hannink RH, Pascoe RT (1975) Ceramic steel? *Nature* 258(5537):703–704. <https://doi.org/10.1038/258703a0>
 62. Heuer AH, Lange FF, Swain MV, Evans AG (1986) Transformation toughening: an overview. *J Am Ceram Soc* 69(i-iv):i–iv. <https://doi.org/10.1111/j.1151-2916.1986.tb07400.x>
 63. Kelly JR, Denry I (2008) Stabilized zirconia as a structural ceramic: an overview. *Dent Mater* 24(3):289–298. <https://doi.org/10.1016/j.dental.2007.05.005>